Creep Along Weak Planes in Roof and How It Affects Stability

by

Mark K. Larson and Ryan G. Wade
National Institute for Occupational Safety and Health, Spokane, WA, USA

ABSTRACT

Researchers at the National Institute for Occupational Safety and Health (NIOSH) are studying the time-dependent response of rock stressed along weakness planes. The objective is to improve mine safety by reducing the number of roof falls that cause injuries and fatalities to miners.

Researchers conducted direct-shear tests on mudstone overcored from a coal mine roof. Results showed frictional strength weakens with displacement along the shearing planes. Results of direct-shear creep tests also showed time-dependent deformation. Test measurements were compared to classical analytical models. Results suggest that risk of roof collapse may be decreased through layout and support design to reduce creep rates and thus slow progression toward failure.

INTRODUCTION

It is an accepted fact that after the initial excavation of an entry, most coal-measure rocks deform over time, even when no mining is taking place nearby. This deformation is most evident in the form of roof sag, floor heave, or pillar dilation, but miners have observed shearing along bedding planes and joints. Time-dependent deformation and strength along joints significantly affect stand-up time of entries (Fakhimi, 1992). In addition, time-dependent mechanisms are evident in the timing of coal bumps. Thus, mine operators cannot ignore rock deformation over time when the risk of a roof fall or a significant amount of entry closure or encroachment are great during the life span of an entry.

NIOSH researchers are interested in learning how to design entries and use support methods that will successfully arrest or delay the onset of instability and resulting roof falls, thereby preventing accidents and fatalities. In this regard, a knowledge of the time-dependent properties of rock is important.

NIOSH researchers have conducted direct-shear, constant-velocity tests and direct-shear creep tests on mudstone cores 152 mm [6 in] in diameter. The cores were collected from the roof of a western U.S. coal mine near a site where Larson and others (1995) measured roof sag over time. Test objectives were to measure friction and creep characteristics of weak planes in the mudstone. The purpose of this paper is to report upon and interpret the results of these tests for engineers who design mine layouts. Simple rheological and constitutive models are used to achieve this goal.

LITERATURE SURVEY

Creep behavior

Maranini and Brignoli (1999) conducted uniaxial, triaxial, and hydrostatic tests (both standard tests and creep tests) to characterize the behavior of Pietra Leccese, a massive unfractured limestone. The predominant deformation mechanisms were crack propagation (at low confining pressures) and pore collapse (at higher stresses). During creep tests, the collapse of pores caused lowering of the yield stress, both in triaxial and hydrostatic configurations.

Price (1964) conducted bending and compressive creep tests on various sandstones, a siltstone, and a nodular muddy limestone. He showed that a Bingham-Voigt model adequately described results of the bending tests. Using the results of Price's bending tests on Pennant Sandstone, Boukharov and others (1995) used rheological models for each phase of creep and applied the models to describe beam deflection over time.

Price's tests comprise the most extensive work done yet on coal-measure rock. However, tests on other rocks should not escape mention. Wawersik (1974) tested intact and jointed rock specimens (Westerly Granite and Navaho Sandstone) in uniaxial and triaxial compression. Creep of the rock was observed, particularly when water was present. Very little creep was seen in a specimen with a clean, interlocked joint. Based on this, Wawersik concluded that the creep behavior of jointed rock has the same character as that of the intact material, but with a larger amount of strain.

Considering Wawersik's statement and the large strains required to account for the amount of roof sag observed in some coal mines, it is likely that creep in brittle coal-measure rock occurs because of (1) microcracking along weak bedding planes and (2) weakening of asperities of

joints. Because of the very friable nature of the mudstone analyzed in this study along bedding, it appears reasonable to conceptualize the shear plane in the mudstone as a cohesive quasi-joint. For a joint, it is important to determine frictional properties in addition to creep characteristics.

Amadei (1979) and Amadei and Curran (1980) conducted direct-shear and triaxial tests on unfilled clean joints sawn in specimens of sandstone, limestone, marble, and granite. They reported that shear displacement was of the form

$$\Delta u_s(t) = A \log_{10}(t + 1) + B + Ct \qquad (1)$$

where *A, B,* and *C* are constants that depend on the ratio of applied shear stress to peak shear strength (for constant normal stress), properties of the intact rock, and joint surface conditions, respectively.

Solberg and others (1978) conducted triaxial tests on Westerly Granite with saw-cut joints filled with crushed Westerly Granite. A confining pressure of 400 MPa (58,000 psi) was applied. They observed a correlation between differential stress and creep rate. Above a differential stress of 1,083 MPa (157,100 psi), primary and secondary creep were followed by tertiary creep and violent slip.

Höwing and Kutter (1985) conducted a study of the effects of joint filler on creep behavior. Creep velocity during the primary phase followed a power law. Creep progressed from the primary to the tertiary phase.

Friction laws

Bowden and Tabor (1964) defined the coefficient of friction as the ratio between shear stress, σ_s, and normal stress, σ_n,

$$\sigma_s = C_o + \mu\sigma_n \qquad (2)$$

in line with Amonton's definition. The Coulomb law in which C_o is inherent joint cohesion and μ is coefficient of friction is supported by Jaeger (1959) and by experiments of Byerlee (1978). Other well-known definitions of frictional strength are provided in Barton (1974) and Ladanyi and Archambault (1970).

Most other friction laws can be placed in one of three classes: displacement weakening, velocity-dependent (velocity weakening), or normal-stress-dependent (normal stress weakening).

The displacement weakening class includes laws such as Patton's (1966) bilinear model, Jaeger's (1959) variation of that model that provides a smooth transition between linear segments, and Cundall and Hart's (1984) continuously yielding joint model that was described further by Cundall and Lemos (1990). In the latter paper, a bounding shear strength was used that was incrementally reduced as shear displacement continued.

Several researchers have suggested or used plasticity models with a nonassociated flow rule to model joint friction and implement a softening law (e.g., Michalowski and Mróz, 1978; Plesha 1987; Fakhimi, 1992; Lofti and Shing, 1994; Mróz and Jarzębowski, 1994; Jarzębowski and Mróz, 1994; Mróz and Giambanco, 1996). Softening is usually dependent on the amount of frictional work done.

Lippmann (1990) discussed the role of friction between a coal seam and overlying and underlying rock layers in the occurrence of translational coal bumps. Detonations, earthquakes, or other seismic events may generate waves along interfaces and thus may convert static friction to sliding friction.

Almost all research in velocity-dependent friction laws is associated with the study of friction along faults. Dieterich's direct-shear experiments on granodiorite (1979) showed that competing time, displacement, and velocity effects control overall friction of a specimen, and so he proposed a simple law. Others (Dieterich, 1981; Ruina, 1983; Rice, 1983; Rice and Ruina, 1983) have proposed various state-variable friction laws. Generally, these laws describe a velocity-dependent friction with transitions over time between friction levels.

Only limited studies and discussions about the effects of normal stress changes on friction have been published. Results of some experiments do not show any effects of normal stress history (Olsson, 1987b; Lockner and Byerlee, 1986), while others do (Hobbs and Brady, 1985; Olsson, 1985, 1987a, 1987b, 1988; Linker and Dieterich, 1986).

Given the nature of mining problems, velocity and normal stress dependence are likely to be second-order effects. Displacement dependence will likely be more significant.

APPARATUS AND EXPERIMENTAL PROCEDURE

All tests were carried out with a Gilmore direct-shear test machine. Each of the two axes has a capacity of 1.334 MN (300,000 lb) and is controlled through a servo-loop with an MTS Teststar II controller. NIOSH engineers designed new specimen boxes (figure 1) for 152-mm (6-in) diameter specimens to accommodate more instruments. Displacement transducers were mounted on the sides of the specimen boxes to measure shear displacement. The average of the

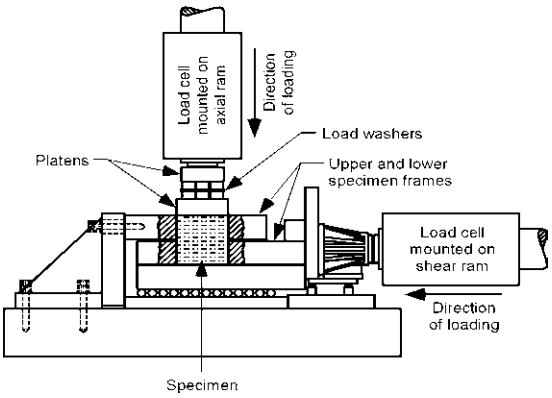

Figure 1.—Sketch of direct-shear test apparatus. Specimen frames are cut away near the specimen for clarity.

two sensors was used as feedback during stroke-controlled test segments.

Two classes of direct-shear tests were done. Constant-load (normal and shear) tests were performed to measure shear displacement over time. Constant-shear velocity tests were done to measure deterioration of the applied shear force and thereby infer reduction of friction on the shearing plane. For one of the constant-shear velocity tests, the velocity was changed suddenly in an attempt to measure any velocity effects. No similar tests were performed to measure the effect of changing normal loads.

Ends of the cores were not ground parallel because of the fragile nature of the rock. The cores were sawn only when the length exceeded the total height of the specimen frames and the shear-plane gap (158.75 mm [6.25 in]). The diameter of the specimen cavity in the steel specimen frames was 155.58 mm (6.125 in), which left a 1.6-mm (0.0625-in) space between the rock and the frames. This space and any space in the frames not taken up by a specimen were filled with Hydrostone Super-X grout and allowed to cure overnight before testing began.

RESULTS

Creep tests

One constant-load, direct-shear creep test was conducted per mudstone core specimen in the first series of tests. In all cases, the first step of the test was to ramp the normal load to the desired level over 60 sec. Next, the shear ram was brought into contact with the specimen frames, and then shear load was ramped to the desired level. The shear and normal loads were held constant over several hours (normally 48) before the shear and normal loads were, in turn, ramped to zero.

Figure 2 shows shear displacement over time for six specimens during the creep portion of the tests. Specimen 02, which failed 5 to 7 min after applying shear load, is also shown in figure 3 with a zoomed-in time scale. This specimen began to exhibit tertiary-phase creep (leading to failure) before transient (primary phase) creep had faded away. Transient creep was demonstrated by all specimens. It is not possible to conclude that constant-rate (secondary phase) creep was present because the duration of the creep test was too short. However, the amount of roof sag over time measured by Larson and others (1995) near the area where these cores were collected suggested primary-phase creep that was still dying out after 207 days. Figure 2 shows no consistent correlation between creep rate and stress ratio (σ_s/σ_n) or amount of creep and stress ratio.

Additional creep tests were begun, but the specimens failed across the shear plane during ramping of the shear load. Figure 4 shows shear stress versus shear displacement. The $\sigma_{s\,(peak)} / \sigma_n$ ratios for specimens 08, 09, 11, 13, 14, and 15 were 0.369, 0.336, 0.532, 0.942, 0.821, and 0.483, respectively. The wide range of ratios suggests the variable nature of the planes sheared. In some specimens, the plane of shear may have been significantly weaker than in other specimens. If the shearing planes are considered pseudo-joints, then joint cohesion is much greater in some specimens than in others.

Specimens 16 and 17 were subjected to several successive creep tests under conditions of constant normal and shear loads. In each test, the normal and shear loads were held constant for 48 hr and then removed. Normal stresses for all tests on specimens 16 and 17 were 2.068 and 1.379 MPa (300 and 200 psi), respectively. Increasing levels of shear stress were applied for each test (figures 5 and 6). Specimen 16 failed during the last test when the shear load was ramped to 95% of normal load. While testing specimen 17 at a shear-to-normal load ratio of 0.90 (the first test at that ratio), a power outage shut down the hydraulic system. Shear displacement data from the tests suggests that load relief caused by the power outage did not cause damage, such as the formation of a crack. Therefore, specimen 17 was again tested at a stress ratio of 0.90.

Figures 5b and 6b show the chronology of tests for the respective specimens, including time breaks between tests. Examination of figures 5 and 6 shows that the amount of primary-phase creep was greatest when there was a period of several hours where no loads were applied before the test. Shear deformation was measured during several of these relaxation periods. While not shown here, the shear-displacement curves during relaxation have approximately the same shape as the loading curves, but in the opposite direction. When a creep test was started within minutes of completion of the previous creep test, the amount and rate of primary-phase creep were smaller than when a relaxation

Table 1.—Successive shear force levels during creep tests where normal force was held constant

Test series	Successive shear forces during creep segments expressed as a fraction of normal force, F_n
1 (σ_n = 2.758 MPa)	0.01, 0.05, 0.20, 0.35, 0.50, 0.65, 0.80, 0.90
2 (σ_n = 1.379 MPa)	0.01, 0.05, 0.20, 0.35, 0.50, 0.575, 0.65, 0.725, 0.80, 0.85, 0.90
3 (σ_n = 4.137 MPa)	0.01, 0.05, 0.20, 0.35, 0.50, 0.575, 0.65, 0.725, 0.80, 0.85, 0.90

period of several hours preceded the creep test.

Another series of creep tests was conducted on specimen 17 to characterize creep response at low levels of applied shear stress. With normal stress held constant at 2.758 MPa (400 psi), five successive tests were conducted with the shear load equal to $0.45F_n$, $0.50F_n$, 222 N (50 lb), 445 N (100 lb), and 667 N (150 lb). Subsequently, relaxation of shear displacement was measured for a couple of days. While the accuracy of the applied shear loads is poor at such low load levels, observations and measurements made while the test was in progress suggest that the applied shear load was not zero. Figure 7 suggests that shear displacement rates were small but initially nonzero at low load levels. The relaxation curve as displayed uses the beginning point as the datum for convenience. The amount of displacement suggests that some of the displacement locked in from the first two tests ($0.45\ F_n$ and $0.50\ F_n$) had not completely relaxed during the low-level creep tests.

Three series of creep tests were conducted on specimen 17 to further characterize the effect of load levels and relaxation on shear displacement. During these series of tests, normal load was maintained at 2.758, 1.379, and 4.137 MPa (400, 200, and 600 psi) for the entire series. In each series, the shear load was held constant for 48 hr, and then removed for 48 hr. This process was repeated with the shear load increased at each cycle. The sequential shear load levels for each test series are described in table 1. Figure 8 shows shear displacement over time during the entire first series. The figure shows that unrecoverable shear displacement took place at $F_s = 0.65\ F_n$ and above.

Figure 9 shows results from the second series of tests in two parts (separated by a dash-dot line) because a hydraulic interlock stopped the test during the eighth creep segment. The test series was resumed, starting with the seventh creep segment. In these tests, unrecoverable strain was evident when the shear load was as low as $0.35F_n$. In running the third series of tests, three hydraulic interlocks occurred, stopping each test early in the series. Finally, the third series was restarted from the beginning, and the entire series was completed without a problem. Figure 10 shows shear displacement over time during the third series of tests. Unrecoverable shear displacement is clearly evident when the shear load was $0.20F_n$ and above.

Constant-Shear-Velocity Tests

Figure 11 shows applied shear stress with shear displacement for five constant-shear-velocity tests. Table 2 lists normal stress and shearing displacement rates used for each test. Shear stress increased linearly up to a peak load. In three of the tests, the shear stress began to decrease quickly almost immediately after reaching peak stress and then continued to decrease with exponentially decaying rates. In the other two tests, shear stress stayed near the peak value for some time. Shearing was allowed to continue long enough for exponential decay to be apparent in one of the two tests. Results of the test with no applied normal load suggested that an exponential decay of shear stress may be typical even when normal stress is low.

Figure 12 shows results of a test on specimen 10. Normal stress was not constant, but decreased nearly linearly because of a test template error. Changes in shear velocity produced only very minor, if any, effects. The shear-stress versus shear-displacement curve is very much like most of the curves in figure 11. Frictional strength appears to be dominated by displacement-weakening behavior. Cohesion, or interlocking of asperities, may be responsible for those instances in which high peak strength dropped off quickly with increasing shear displacement.

Table 2.—Conditions of constant-rate, direct-shear tests

Specimen	Normal stress		Shearing displacement rate	
	MPa	psi	mm/sec	in/sec
01	1.724	250	0.038100	0.001500
05	1.724	250	0.009525	0.000375
06	2.758	400	0.038100	0.0015
07	0	0	0.038100	0.0015
10	1.724	250	0.009525	0.000375
			0.038100	0.001500
			0.009525	0.000375
			0.002381	0.000094
13	2.758	400	0.009525	0.000375

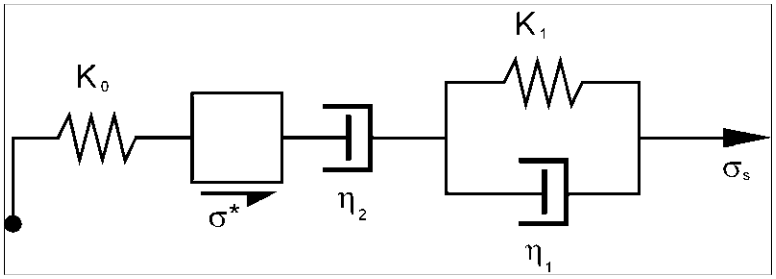

Figure 13.—Rheological model used to examine behavior during creep test

MODELS

A preliminary comparison with analytical models will provide some insight into results of laboratory tests on mudstone. Figure 13 shows elements of a rheological model (essentially the same as that used by Boukharov and others, 1995) that may reasonably account for the deformation measured. For this model, shear displacement may be represented by

$$u_s = \frac{\sigma_s}{K_0} + \frac{\sigma_s}{K_1}\left(1 - e^{\frac{-tK_1}{\eta_1}}\right) + \frac{H(\sigma_s - \sigma^*)\,(\sigma_s - \sigma^*)\,(t - t^*)}{\eta_2}, \quad (3)$$

where u_s is shear displacement, σ^* is a strength above which constant-rate creep takes effect, t is time, t^* is the time when $\sigma_s \geq \sigma^*$, $H(\sigma_s - \sigma^*)$ is the Heaviside step function (= 1 when its argument, $\sigma_s - \sigma^*$, ≥ 0; otherwise, = 0), K_0 and K_1 are stiffness parameters, and η_1 and η_2 are viscosity parameters.

Figure 14 compares shear displacement over time from figure 8 with model calculations using equation 3 with estimated (only one creep curve was fitted) parameters. The reader should note that the last term of equation 3 was reset for each loading step, but previously accumulated displacements from that term were left in the total shear displacement. In the calculations, K_0 was 4.34315 MPa/mm (16,000 psi/in), K_1 was 106.0232 MPa/mm (390,585.3 psi/in), η_1 was 6,251,726 MPa·t/mm (2.3031099×10^{10} psi·t/in), η_2 was 5,428,943 MPa·t/mm (2.000000×10^{10} psi·t/in), and σ^* was 1.600 MPa (232 psi)—58% of the applied normal stress. For the figure, a seating displacement of 0.01778 mm (0.0007 in) was assumed. Comparison of the model curve with measured results suggests that transient creep in the specimen may not have depended on shear stress level as much as did transient creep in the model. The model was able to capture the unrecoverable shear displacement above some level, similar to the measured result. Displacement offsets were not always well simulated with the K_0 stiffness in the model, suggesting a degree of nonlinearity of the specimen in the elastic region. At higher shear stresses, the shear stiffness began to soften.

Figure 15 compares shear displacement over time from figure 11 with model calculations using

$$S_s = C + \sigma_n \tan\phi \quad (4)$$

where S_s is shear strength, C is cohesive strength, and

$$\phi = \phi_{res} + (\phi_p - \phi_{res})\left(1 - e^{-\alpha(u_s - u^*)}\right). \quad (5)$$

In equation 5, ϕ is friction angle, ϕ_{res} is residual friction angle, ϕ_p is peak friction angle, u^* is shear displacement when $\sigma_s = S_s$, and α is empirical constant. In the model calculations, parameters were estimated—σ_n was 2.758 MPa (400 psi), C was 2.413 MPa (350 psi), ϕ_{res} was 1°, ϕ_p was 6.4°, and α was 0.031496 mm^{-1}. The shear stiffness in the calculations for the loading portion of the curve was 2.8366 MPa/mm (10,450 psi/in). The model's failing is that the cohesion assumed the value of zero when the shear stress reached the shear strength. However, cohesion in the specimen did not reach zero as quickly. The jagged loss-of-cohesion effect actually may be the result of relatively large asperities that were sheared off, although not all at once. Perhaps a cohesion-like parameter may be appropriate if it decreases exponentially with shear displacement instead of going to zero suddenly when the shear strength is exceeded. The absence of sharp peaks in some of the test results (in figure 11) suggests that larger asperities may not always be intact or present. It may be more appropriate to model such behavior with a dilation angle that deteriorates with shear displacement.

DISCUSSION

Results thus far suggest some points to be considered when a mine operator is concerned about long-term stability of entries. In this regard, the authors have assumed that joints and planes of weakness play a dominant role in roof sag. The similarities in creep behavior (transient creep) between tested core and roof sag over time (Larson and others, 1995) suggest that behavior measured in the laboratory is relevant to the field. It is interesting to note that Larson and Maleki (1996) measured constant-rate roof sag in a different part of the mine where roof conditions were not as uniform. Constant-rate deformation was pronounced at this second measurement site. The differences in roof sag over time suggests that a knowledge of creep properties and design principles may be used to prevent collapse during the service life of the opening. One way to do that is to design entries so that constant-rate creep is reduced or entirely avoided. This approach doesn't preclude the possibility of collapse, but if the amount of creep over time can be reduced, the probability of collapse during an entry's service life decreases.

If the rheological model is valid (i.e., constant-rate creep along weakness planes occurs only when shear stress is above some strength σ^*), then it may be possible to design entries so that shear stress along bedding is maintained below strength σ^*. This may be achieved with roof support; however, care must be exercised in the case of bolts and cable bolts so that applied shear stress does not exceed the shear strength of the bolts (Signer and Lewis, 1998; McHugh and Signer, 1999). Where shear stress is kept below σ^*, roof sag would tend to stabilize unless transient creep is large enough that σ^* might significantly decrease. It is not known if σ^* is dependent on normal stress, but test results suggest that its weakening is dependent on total shear displacement or damage. Another possibility is that σ^* decreases by static fatigue (Larson, 1998), which is suggested by the failure of specimen 02 (figure 3).

The combination of equations 4 and 5 seems a reasonable approximation to shear strength. However, it may be appropriate to include in equation 4 a dilation angle that decreases with shear displacement.

The next logical step is to write code for such constitutive models (equations 3, 4, and 5) in a numerical model and examine how well laboratory tests or measured roof sag deformation can be simulated. Some of the unanswered questions might be resolved by accomplishing this step.

CONCLUSIONS AND RECOMMENDATIONS

Comparing the results of direct-shear laboratory tests with field measurements of roof sag suggests that knowledge of characteristic creep behavior of planes of weakness in mudstone can be useful in the design of stable long-term entries so that roof collapse is avoided. This might be accomplished by designing entries and support in such a way to reduce the rate or avoid the onset of secondary-phase creep.

Primary-phase creep was seen along planes of weakness in the mudstone even at low shear stresses, but unrecoverable or secondary-phase creep only took place when shear stresses were above a certain level. That strength decreased with further testing of the specimen.

It is recommended that the models used in this report be coded into a numerical model to investigate their applicability in laboratory tests and field case histories.

REFERENCES

Amadei, B. 1979. *Creep Behaviour of Rock Joints*. M. App. Sc. thesis, Univ. Toronto, 227 pp.

Amadei, B., and J. H. Curran. 1980. Creep behavior of rock joints. In *Underground Rock Engineering: 13th Canadian Rock Mechanics Symposium* (H. R. Rick Memorial Symp., Toronto, ON, May 28-29, 1980). Can. Inst. Min. and Metall., CIM Special Vol. 22, pp. 146-150.

Barton, N. 1974. Estimating the shear strength of rock joints. In *Advances in Rock Mechanics: Reports of Current Research, Themes 1-2. Proceedings of the Third Congress of the ISRM*, (Denver, CO, Sept. 1-7, 1974). Nat. Acad. Sci., Vol. II, Part A, pp. 219-220.

Boukharov, G. N., M. W. Chandi, and N. G. Boukharov. 1995. The three processes of brittle crystalline rock creep. *Int. J. Rock Mech. Min. Sci. & Geomech. Abstr.*, Vol. 32, No. 4, pp. 325-335.

Bowden, F. P., and D. Tabor. 1964. *The Friction and Lubrication of Solids, Part II*. Oxford University Press, 566 pp.

Byerlee, J. 1978. Friction of rocks. *Pageoph*, Vol. 116, pp. 615-626.

Cundall, P. A., and R. D. Hart. 1984. Analysis of block test no. 1 inelastic rock mass behavior–phase 2: A characterization of joint behavior (final report). Itasca

Consulting Group Report, Rockwell Hanford Operations, Subcontract SA-957, 37 pp.

Cundall, P. A., and J. V. Lemos. 1990. Numerical simulation of fault instabilities with the continuously-yielding joint model. In *Rockbursts and Seismicity in Mines: Proceedings of the 2nd International Conference on Rockbursts and Seismicity in Mines*, ed. by C. Fairhurst (Minneapolis, MN, June 1988). Balkema, pp. 147-152.

Dieterich, J. H. 1979. Modeling of rock friction 1. Experimental results and constitutive equations. *Journal of Geophysical Research*, Vol. 84, No. B5, May 10, pp. 2161-2168.

Deiterich, J. H. 1981. Constitutive properties of faults with simulated gouge. In *Mechanical Behavior of Crustal Rock*. American Geophysical. Union Monograph, Vol 24, pp. 103-120.

Fakhimi, A. A. 1992. *The Influence of Time Dependent Deformation of Rock on the Stability of Underground Excavations*, Ph. D. thesis, Univ. Minnesota, 186 pp.

Hobbs, B. E.. and B. H. G. Brady. 1985. Normal stress changes and the constitutive law for rock friction. *Eos, Transactions of the American Geophysics Union*, Vol. 66, No. 18, April 30, p. 382.

Höwing, K. D., and H. K. Kutter. 1985. Time-dependent shear deformation of filled rock joints. A keynote lecture in fundamentals of rock joints. In *Proceedings of the International Symposium on Fundamentals of Rock Joints*. (Björkliden, Sept. 15-20, 1985). Centek Publishers, pp. 113-122.

Jaeger, J. C. 1959. The frictional properties of joints in rocks. *Geofisica Pura e Applicata*, Vol. 43, pp. 148-159.

Jarzębowski, A., and Z. Mróz. 1994. On slip and memory rules in elastic friction contact problems. *Acta Mechanica*, Vol. 102, No. 1-4, pp. 199-216.

Ladanyi, B., and G. Archambault. 1970. Simulation of shear behavior of a jointed rock mass. In *Rock Mechanics—Theory and Practice: Proceedings, Eleventh Symposium on Rock Mechanics* (Berkeley, CA,. June 16-19, 1969) Society of Mining Engineers of AIME, pp. 105-125.

Larson, M., K. 1998. A static fatigue constitutive law for joints in weak rock. In *Proceedings of the Third International Conference on Mechanics of Jointed and Faulted Rock*, ed. by H. P. Rossmanith (Vienna, Austria, April 6-9, 1998). Balkema, pp. 171-177.

Larson, M. K,. and H. Maleki. 1996. Geotechnical factors influencing a time-dependent deformation mechanism around an entry in a dipping seam. In *Proceedings, 15th International Conference on Ground Control in Mining* ed. by L. Ozdemir, K. Hanna, K. Y. Haramy, and S. Peng (Golden, CO, Aug 13-15, 1996). Colorado School of Mines, pp. 699-710.

Larson, M. K., C. L. Stewart, M. A. Stevenson, M. E. King, and S. P. Signer. 1995. A case study of a deformation mechanism around a two-entry gate-road system involving probable time-dependent behavior. In *Proceedings of the Fourteenth Conference on Ground Control in Mining*, ed. by S. Peng (Morgantown, WV, Aug 1-3, 1995). Dept. of Min. Eng., WV. Univ., pp. 295-304.

Linker, M. F., and J. H. Dieterich. 1986. Effects of variable normal stress on rock friction: Observations at 50 bars normal stress. *Eos, Transactions of the American Geophysics Union*, Vol. 67, p. 1187.

Lippmann, H. 1990. Mechanical considerations of bumps in coal mines: Keynote lecture. In *Rock bursts and Seismicity in Mines: Proceedings of the 2nd International Conference on Rockbursts and Seismicity in Mines*, ed by C. Fairhurst (Minneapolis, MN, June 1988). Balkema, pp. 279-284.

Lockner, D. A., and J. D. Byerlee. 1986. Laboratory measurements of velocity-dependent frictional strength. U.S. Geological Survey, Open File Report 86-417, 55 pp.

Lofti, H. R., and P. B. Shing, 1994. Interface model applied to fracture of masonry structures. *Journal of Structural Engineering*, Vol. 120, No. 1, pp. 63-80.

Maranini, E., and M. Brignoli. 1997. Creep behavior of a weak rock: experimental characterization, *Int. J. Rock Mech. Min. Sci.*, Vol. 36, No. 1, pp. 127-138.

McHugh, E., and S. Signer. 1999. Roof bolt response to shear stress: laboratory analysis. In *Proceedings, 18th International Conference on Ground Control in Mining*, ed. by S. Peng and C. Mark (Morgantown, WV, Aug 3-5, 1998). Dept. Of Min. Eng., WV. Univ., pp. 232-238.

Michalowski, R., and Z. Mróz. 1978. Associated and nonassociated sliding rules in contact friction problems. *Archives of Mechanics, Archiwum Mechaniki Stosowanej*, Vol. 30, Issue 3, pp. 259-276.

Mróz, Z., and G. Giambanco. 1996. An interface model for analysis of deformation behavior of discontinuities. *Int. J. Numer. Anal. Methods Geomech.*, Vol. 20, No. 1, pp. 1-33.

Mróz, Z,. and A. Jarzębowski. 1994. Phenomenological model of contact slip. *Acta Mechanica*, Vol. 102, No. 1-4, pp. 59-72.

Olsson, W. A. 1985. Normal stress history effects on friction in tuff. *Eos, Transactions of the American Geophysics Union*, Vol. 66, p. 1101.

Olsson, W. A. 1987a. The effects of changes in normal stress on rock friction. In *Constitutive Laws for Engineering Materials—Theory and Applications*, ed. by S. Desai, E. Krempl, P. D. Kiousis, and T. Kundu. Elsevier, p. 1059-1066.

Olsson, W. A. 1987b. Rock joint compliance studies. Sandia National Laboratories Report, Sand86-0177, 103 pp.

Patton, F. D. 1966. Multiple modes of shear failure in rock. In *Proceedings of the First Congress of the International Society of Rock Mechanics* (Lisbon, Sept. 25 - Oct 1, 1966). Bertrand (Irmãos), Vol. I, pp. 509-513.

Plesha, M. E. 1987. Constitutive models for rock discontinuities with dilatancy and surface degradation. *Intern. J. Numer. Anal. Methods Geomech.*, Vol. II, pp. 345-362.

Price, N. J. 1964. A study of time-strain behavior of coal-measure rocks. *Int. J. Rock Mech. Min. Sci. & Geomech. Abstr.* 1(2):277-303.

Rice, J. R. and A. L. Ruina. 1983. Stability of steady frictional slipping. *J. of Applied Mechanics*, Vol. 50, June, pp. 343-349.

Rice, J. R. 1983. Constitutive relations for fault slip and earthquake instabilities. *Pageoph*, Vol. 121, No. 3, pp. 443-475.

Ruina, A. 1983. Slip instability and state variable friction laws. *J. of Geophysical Research*, Vol. 88, No. B12, Dec. 10, pp. 10359-10370.

Signer, S. P., and J. L. Lewis. 1998. A case study of bolt performance in a two-entry gateroad. In *Proceedings, 17th International Conference on Ground Control in Mining*, ed. by S. Peng (Morgantown, WV, Aug 4-6, 1998). Dept. of Min. Eng., WV. Univ., pp. 249-256.

Solberg, P. H., D. A. Lockner, R. S. Summers, J. D. Weeks, and J. D. Byerlee. 1978. Experimental fault creep under constant differential stress and high confining pressure. Preprint, *Proceedings, 19th U.S. Symposium on Rock Mechanics* (Stateline, NV, May 103, 1978). Univ. of Nevada-Reno, pp. 118-120.

Wawersik, W. R. 1974. Time-dependent behavior of rock in compression. In *Advances in Rock Mechanics: Reports of Current Research, Themes 1-2. Proceedings of the Third Congress of the International Society for Rock Mechanics*. Nat. Acad. Sci., Vol. II, Part A, pp. 357-363